EBioMedicine 33 (2018) 22–32

Contents lists available at ScienceDirect

EBioMedicine

journal homepage: www.ebiomedicine.com

Research Paper

Proapoptotic Cyclic Peptide BC71 Targets Cell-Surface GRP78 and Functions as an Anticancer Therapeutic in Mice

Chieh Kao [a], Ritu Chandna [a], Abhijeet Ghode [a], Charlotte Dsouza [a], Mo Chen [a], Andreas Larsson [b], Siau Hoi Lim [b], Minjun Wang [c], Zhonglian Cao [c], Yizhun Zhu [c], Ganesh S. Anand [a], Ruowen Ge [a,*]

[a] Department of Biological Sciences, National University of Singapore, 16 Science Drive 4, 117558, Singapore
[b] School of Biological Sciences, Nanyang Technological University, 60 Nanyang Drive, 639798, Singapore
[c] School of Pharmacy, Fudan University, 826 Zhangheng Rd, Shanghai 201203, China

ARTICLE INFO

Article history:
Received 2 March 2018
Received in revised form 25 May 2018
Accepted 6 June 2018
Available online 12 June 2018

ABSTRACT

Glucose regulated protein 78 kDa (GRP78) is a recently emerged target for cancer therapy and a biomarker for cancer prognosis. Overexpression of GRP78 is observed in many types of cancers, with the cell-surface GRP78 being preferentially present in cancer cells and cancer blood vessel endothelial cells. Isthmin (ISM) is a secreted high-affinity proapoptotic protein ligand of cell-surface GRP78 that suppresses angiogenesis and tumor growth in mice. The C-terminal AMOP (adhesion-associated domain in MUC4 and other proteins) domain of ISM is critical in mediating its interaction with human umbilical vein endothelial cells (HUVECs). In this work, we report novel cyclic peptides harboring the RKD motif in the ISM AMOP domain that function as proapoptotic ligands of cell-surface GRP78. The most potent peptide, BC71, binds to GRP78 and converge to tumor in mice. Intravenous administration of BC71 suppressed xenograft tumor growth in mice as a single agent, with significant reduction in tumor angiogenesis and upsurge in apoptosis. Fluorescent-labeled BC71 accumulates in tumor in mice by targeting cell-surface GRP78. We show that BC71 triggers apoptosis via cell-surface GRP78 and activates caspase-8 and p53 signaling pathways in HUVECs. Using amide hydrogen-deuterium exchange mass spectrometry (HDXMS), we identified that BC71 preferentially binds to ATP-bound GRP78 via amino acid residues 244–257 of GRP78. Hence, BC71 serves as a valuable prototype for further development of peptidomimetic anticancer drugs targeting cell-surface GRP78 as well as PET imaging agents for cancer prognosis.

1. Introduction

GRP78 is a member of the heat-shock protein family and a major endoplasmic reticulum (ER) chaperone protein which modulate protein folding. It is a stress-response protein whose expression is up-regulated in cells under stress. Cancer cells are under constant stress caused by their microenvironment of hypoxia, acidity and metabolic toxicity. It has been reported that GRP78 is overexpressed in various human cancers including breast cancer, prostate cancer, lung cancer, ovarian cancer, and melanoma. Overexpression of GRP78 in cancer is linked to chemoresistance, increased malignancy, and poor patient outcomes [16, 17, 25].

Overexpression of GRP78 leads to its translocation to the cell-surface in cancer cells and cancer blood vessel ECs. Cell-surface GRP78 has been shown to function as a receptor for proapoptotic ligands such as Kringle-5 and Par-4, mediating apoptosis [21, 28]. Phage-display library screening has identified several synthetic peptides that bind to cell-surface GRP78 [1, 12]. Conjugation of a proapoptotic peptide to a GRP78 binding peptide resulted in a GRP78-targeting proapoptotic peptide that potently suppressed tumor growth in mice [22]. Meanwhile, anti-GRP78 monoclonal antibodies also function as potent anticancer therapeutics in mice or human clinical trials [18, 23, 24]. Nevertheless, no anticancer therapeutics targeting GRP78 have reached the clinics as of now.

GRP78 is overexpressed in both cancer cells and cancer blood vessel endothelial cells (ECs) [4, 26, 31]. Excessive angiogenesis and resistance to apoptosis are two hallmarks of cancer [9]. Inducing EC apoptosis can suppress angiogenesis and induce vessel regression, thus is a useful strategy for antiangiogenic cancer therapy [34]. Meanwhile, inducing cancer cell apoptosis has also been actively pursued in anticancer therapeutic development [5, 7, 11].

Isthmin (ISM) is a secreted proapoptotic protein recently identified by us [36]. It contains two important domains, a central thrombospondin type I repeat (TSR) domain and a C-terminal AMOP (adhesion associated

Abbreviations: GRP78, Glucose regulated protein 78 kDa; ISM, Isthmin; AMOP, Adhesion-associated domain in MUC4 and other proteins; HUVECs, Human umbilical vein endothelial cells; TSR, Thrombospondin type I repeat; ER, Endoplasmic reticulum.

* Corresponding author.
E-mail address: dbsgerw@nus.edu.sg (R. Ge).

https://doi.org/10.1016/j.ebiom.2018.06.004

domain in MUC4 and other proteins) domain. Bacterially expressed recombinant ISM (rISM) induced human umbilical vein endothelial cell (HUVEC) apoptosis and suppressed angiogenesis in vitro and in vivo [36]. Cell-surface GRP78 is a high-affinity receptor for ISM (K_d of 8.6 nM) [4]. ISM selectively induces apoptosis in cells harboring high level cell-surface GRP78 including activated endothelial cells and highly metastatic and aggressive cancer cells [4]. As a potent proapoptotic ligand of cell-surface GRP78, ISM has the potential to be a drug specifically targeting chemoresistant and aggressive cancers.

Peptide-based drugs possess several advantages over small molecule drugs including higher target specificity, no accumulation in tissues and organs, less side effects and less long-term toxicity. Compared to recombinant proteins and antibodies, peptides are less immunogenic and potentially cheaper to manufacture [32].

In this study, we report a GRP78-specific cyclic peptide BC71 designed based on the AMOP domain of ISM which induces apoptosis in HUVECs. Systemic delivery of BC71 effectively suppressed subcutaneous tumor growth in mice as a single agent. We show that BC71 accumulates in tumors likely by binding to cell-surface GRP78 overexpressed on the surfaces of tumor cells and tumor blood vessel endothelial cells. Hence, BC71 is a valuable prototype peptide which can be further developed into GRP78-targeted anticancer therapeutic as well as an imaging probe for GRP78 for cancer prognosis.

2. Materials and Methods

2.1. Cell Lines and Reagents

HUVECs were purchased from Lonza and cultured in EndoGro-LS (Millipore, Bradford, MA, USA) supplemented with FBS and gentamycin (Sigma-Aldrich, St. Louis, MO, USA) on pre-coated culture dishes/inserts/slides. All experiments were performed on cells from passages 5–10. 4 T1 cells were purchased from ATCC (Manassas, VA, USA) and cultured in DMEM with 10% FBS (Sigma-Aldrich, St. Louis, MO, USA). Antibodies against integrin αvβ5 (P1F76; Santa Cruz Biotechnology, Santa Cruz, CA, USA), GRP78 (A-10, Santa Cruz Biotechnology) and GRP78 (C-20, Santa Cruz Biotechnology) were used for neutralization. P53 inhibitor (Pifithrin-α hydrobromide, PFT-α sc-45050A) and caspase-8 inhibitor (z-IETD-fmk, sc-3084) were purchased from Santa Cruz Biotechnology. Synthetic ISM-related peptides were synthesized by Ontores (Hangzhou, China), Mimotopes (Melbourne, Australia) and China Peptide (Shanghai, China). The Cy7 labeled peptides was synthesized by Cambridge Research Biochemicals Limited (Cleveland, UK).

2.2. Cell Viability Assay

HUVECs were plated at 5×10^3–1×10^4 cells per well of 96-well plates and were treated with 100 μM ISM peptide in 2% FBS EndoGro medium for 24 h or 48 h before being used in the assays. The inhibitory effects of ISM peptide on the growth of HUVECs were measured by the MTT (3-(4,5-dimethylthiazol-2-yl)-2,5-diphenyltetrazolium bromide) method (Sigma-Aldrich, St. Louis, MO, USA). The optical density was measured at 570 nm using an automated scanning multiwall spectrophotometer.

2.3. Lactate Dehydrogenase (LDH) Assays

The cytotoxicity of ISM-peptide on HUVECs was investigated. Cells were plated at 5×10^3–1×10^4 cells per well of 96-well plates and treated with 100 μM ISM peptide in 2% FBS EndoGro medium for 24 h or 48 h before being used in the assays. To calculate the activity of LDH, 100 μl of a reaction mixture (Cytotoxicity Detection Kit; Sigma-Aldrich, St. Louis, MO, USA) and the conditional medium were added to each well and incubated in the dark for 10–30 min. The water-soluble formazan dye exhibited the broad absorption maximum at approximately 490 nm in the spectrophotometer.

2.4. Cell Death ELISA Assay

HUVECs were seeded at 1–1.5×10^4 cell per well of 96-well plates and were co-treated with 100 μM ISM peptide +15 ng/ml VEGF and 5, 10, 20 μM z-IETD-fmk or 7.5, 15, 30 μM PFT-α, or pretreated with anti-GRP78 antibody for 60 min after pre-starved in 2% FBS medium for 3 h. The Cell Death Detection ELISA photometric enzyme immunoassay (Sigma-Aldrich, St. Louis, MO, USA) was used for the quantitative in vitro determination of cytoplasmic histone-associated DNA fragments (mono- and oligonucleosomes) as an indicator of apoptosis. The absorbance was measured at 405 nm.

2.5. ATP Colorimetric Assay

The ATP concentrations in whole-cell lysate, mitochondrial and cytosolic (without mitochondria) fractions in HUVECs with indicated treatment of 100 μM BC71 for 24 h, were analyzed using the ATP colorimetric assay kit (BioVision, Milpitas, CA, USA).

2.6. Surface Plasmon Resonance (SPR) Binding Assays

The experiments were performed using a BIACORE T200 instrument (GE healthcare) equipped with research-grade NTA-S sensor chip. GRP78 protein was immobilized using the capture-coupling method performed by a slight modification of the method as described previously [33]. The surfaces of flow cells 1 and 2 were activated for 3 min with 0.5 mM $NiCl_2$, followed by 7 min with a 1:1 mixture of 0.1 M NHS and 0.1 M EDC and finally by 1 min 0.5 mM $NiCl_2$ at a flow rate of 5 μl/min. The ligand, GRP78 at a concentration of 60 μg/ml in 10 mM sodium acetate, pH 6.0, was immobilized at a density of 2500–3000 RU on flow cell 2; flow cell 1 was left blank to serve as a reference surface. All the surfaces were blocked with a 7 min injection of 1 M ethanolamine, pH 8.0 and washed for 2 min with 0.35 M EDTA solution.

Peptides of interest (the analytes) dissolved or exchanged into HBS-EP buffer (10 mM HEPES, 150 mM NaCl, 3 mM EDTA 0.005% P20, pH 7.4), and injected over the two flow cells at a flow rate of 30 μl/min and at a temperature of 25 °C. Data were collected at a rate of 1 Hz. Each sample series consisted of single injections of the analyte at 1.25 μM and 200 μM followed by duplicate injections of buffer blank to allow double referencing. The complexes were allowed to associate for 30 s and dissociate for 120 s and the surfaces were regenerated with a 60 s injection of a 1:1 mixture of 20 mM sodium hydroxide and running buffer. The binding data were analyzed and fitted using the software Scrubber 2.0 (BioLogic software). At higher concentrations many of the peptides exhibited problematic injections likely due to low solubility or aggregation so a full, saturated isotherm couldn't be recorded in many cases. To ensure fair comparability of the different peptides and a good relative ranking we fitted RU_{max} globally which was then used in the subsequent steady-state fits of the peptides.

2.7. HDXMS

Recombinant GRP78 ATPase domain (26–410) was expressed and purified in *E. coli* as previously described [35] and reconstituted in buffer A (20 mM Tris, pH 7.5, 150 mM NaCl, 5% glycerol, 5 mM DTT). Stock ADP and AMPPNP (Sigma-Aldrich, St. Louis, MO, USA) solutions at 4.8 mM were prepared in buffer A with 2 mM Mg^{2+} added. Lyophilized BC71 peptide was dissolved in autoclaved deionized water, and its pH adjusted to ~7.5. For pepsin fragment peptides identification, aqueous samples (undeuterated reactions), were diluted in buffer A, and a quench solution prepared using trifluoroacetic acid (TFA) and 1 M Gn-HCl was added to bring final pH to 2.5. Deuterium exchange reactions were initiated with buffer A reconstituted in 99.9% D_2O to generate a final D_2O concentration of 90% followed by incubation at 25 °C for different time points (t = 0.5, 1, 5, 10 and 100 mins). Deuteration reactions were quenched with pre-chilled quench solution. Samples were

injected onto nanoACQUITY UPLC system (Waters, Milford, MA, USA) and subject to online pepsin proteolysis by Poroszyme immobilized pepsin column (Life Technologies Corp, Bedford, MA, USA), with LC separation of the digested peptides on an ACQUITY UPLC BEH C18 reversed-phase column and detected by a SYNAPT G2-*Si* high-definition mass spectrometer (Waters, Manchester, UK) operating in MS^E data acquisition mode. Peptides were identified from the undeuterated reactions using ProteinLynx Global Server software (PLGS 3.0.1, Waters) using the sequence of GRP78 (26–410) as a search database for peptide identification by matching observed masses obtained from the experiment to the expected masses of theoretical proteolytic peptides cleaved by a nonspecific protease. The list of fragment peptides identified by PLGS was imported into deuterium exchange analysis program DynamX 3.0 (Waters) and filtered using the following cutoffs for the different parameters as specified: A minimum signal intensity of 2000, minimum product ions per amino acid of 0.1, maximum MH+ error of 10 ppm, and a minimum of 6 replicates out of total 19 undeuterated reactions containing the peptide. Peptides were found to be within 25 residues in size. This software was then used to guide assignment of mass spectra, calculate peptide-level deuterium uptake, and to generate uptake profiles and difference plots to compare deuterium exchange under different reaction conditions.

2.7.1. In Vivo Near Infrared (NIR) Whole Mouse Fluorescent Imaging

Mouse procedures were performed according to IACUC protocol R16-0632 approved by the National University of Singapore Institutional Animal Care and Use Committee. Female Balb/cAnNTac mice were obtained from InVivos (Singapore) at 7–8 weeks of age. Mouse breast cancer 4 T1 cells (1×10^6 cells/mouse) were injected subcutaneously in the upper right foreleg region. When the tumors reached 0.6 to 0.8 cm in diameter (12–14 days after implant), the tumor-bearing mice were subjected to in vivo imaging studies. In vivo NIR fluorescence imaging was performed with Xenogen IVIS™ 200 small animal imaging system (Xenogen, Alameda, CA) with a Cy7 filter set (excitation: 745/30 nm; emission: 800/30 nm). The surface fluorescence intensity of the animal was measured and normalized to photons per second per centimetre squared per steradian (p/s/cm2/sr). Mice were injected via tail vein with 1 nmol of Cy7-BC71 or Cy7-GR35 or Cy7 dye/mouse (n = 5 for all 3 groups), anesthetized with 2–3% isoflurane (Abbott Laboratories), and imaged at various time points post-injection (p.i.). The tumors and major organs and tissues were dissected at 72 h p.i. and imaged again. The total fluorescence flux (p/s/cm2/sr) for each organ was measured. The average radiant efficiency of all the organs is plotted.

2.8. Mouse Xenograft Tumorigenesis Assay

Mice care and experimentation were carried out according to approved protocol by the University institutional animal care and use committee, which conforms to NIH guidelines (IACUC protocol R16-0632). Only female Balb/cAnNTac mice of ages 5–6 weeks were used in the experiments. 4 T1 cells (5×10^5) were injected subcutaneously into the dorsal flank of 7-week-old female BALB/C mice. Two groups of mice received either PBS or 12.5 mg/kg (250 μg/mouse) BC71 (n = 5) or BC51 (n = 10) through tail vein every other day from day 7 (date of inoculation) to day 23. Tumors were measured and processed for immunostaining as described [13].

2.9. Data Analysis

All of the data are expressed as mean ± standard error of the mean, unless otherwise indicated. The results are representative of at least three independent experiments. Statistical significance was determined using ANOVA. *$P < 0.05$; **$P < 0.01$, $n \geq 3$.

3. Results

3.1. RKD Containing Peptide Analogues Derived from ISM Induces Apoptosis in HUVECs

We have previously shown that the extracellular ISM protein can potently induce EC apoptosis by binding to its cell-surface receptors αvβ5 integrin and GRP78 [4, 37]. We also demonstrated that mutating the critical $KD_{316–317}$ residues to AA in ISM's C-terminal AMOP domain caused the recombinant AMOP polypeptide to lose its ability to support HUVEC adhesion [37]. Based on the sequence surrounding $KD_{316–317}$, we synthesized GR01 and GR16, two small cyclic peptides harboring the core RKD motif encompassing $KD_{316–317}$ in the AMOP domain, and tested their proapoptotic activity towards HUVECs. Both GR01 and GR16 exhibited proapoptotic activities towards HUVECs (Table 1). Mutation of the KD residue to AA in GR16 (GR35) significantly reduced its proapoptotic activity, indicating the importance of these two residues in mediating the proapoptotic activity of these peptides. Based on these two peptides, we further generated a library of modified cyclic peptide analogues. In all, 16 peptide analogues were found to exhibit proapoptotic activities, but only three peptides (BC51, BC71 and BC84) also showed reduced cell viability (Fig. 1, a–c; Table 1). These three more potent peptides all harbor the RKD core sequence, and none of the peptides caused necrosis (Fig. 1, d & e; Table 1). Amongst the three peptides, BC71 exhibited the highest proapoptotic activity towards HUVECs (Fig. 1, b & c; Table 1). Both BC71 and BC51 induced apoptosis of HUVECs in a dose-dependent manner (Fig. 2a; Fig. S1a). We thus selected BC71 for subsequent studies.

3.2. BC71 Induced Apoptosis Via Cell-Surface GRP78, but Not αvβ5 Integrin

ISM acts on HUVECs through both of its cell surface receptors αvβ5 integrin and GRP78. While GRP78 is the high-affinity receptor, αvβ5 integrin is the low-affinity receptor, although both pathways trigger apoptosis [4, 37]. To investigate which receptor mediates BC71's proapoptotic function, we performed antibody neutralization experiments using antibodies against GRP78 and αvβ5 integrin respectively. N-terminal anti-GRP78 antibody dose dependently inhibited BC71-induced apoptosis function but no effect was observed in the case of anti-αvβ5 integrin antibody (Fig. 2b, d and Fig. S1b). Interestingly, anti-GRP78 c-terminal antibody alone induced some apoptosis and but did not show any attenuation of BC71-induced apoptosis (Fig. 2c). Taken together, these results indicate that BC71 induces apoptosis most likely by interacting with the N-terminal region of GRP78.

3.3. BC71 Induces Apoptosis Via Activating Caspase-8 and p53 Signaling Pathway in HUVECs

ISM is known to co-target with GRP78 to mitochondria where it causes the blockade of ATP transport to cytosol, thus causing apoptosis [4]. Cell-surface GRP78 has also been shown to trigger downstream caspase-8 and p53 signaling cascade following extracellular Par-4 binding [28, 30]. To decipher the mechanism of BC71-activated apoptosis, we investigated if BC71 influences Par-4 expression and secretion in HUVECs. As shown in Fig. S1, BC71 treatment of HUVECs did not alter Par-4 expression and secretion. We next examined if BC71 blocks ATP transport to the cytosol, similar to ISM protein. No change in ATP levels was observed in either cytosolic or mitochondrial fractions under BC71 treatment, indicating that this peptide did not affect ATP transport (Fig. 3a). On the other hand, inhibition of caspase-8 (by z-IETD-fmk) and p53 (by PFT-α) both significantly attenuated BC71-mediated apoptosis (Fig. 3, b & c). Moreover, we demonstrated that BC71 can increase p53 expression level and activate caspase-8 (Fig. 3d). Similarly, peptide BC51 also induced HUVEC apoptosis via caspase-8 and p53 pathways (Fig. S2, c & d).

Table 1
Selected ISM-derived peptide analogues.

Peptide name	Sequence	Cyclization	Pro-apoptotic activity	Cell viability
GR01	c[CRKDC]	Disulfide bridge: 1-5	2.14	0.94
GR16	c[KRKDF]	Amide cyclic: 1-5	3.13	0.96
GR35	c[KRAAF]	Amide cyclic: 1-5	1.30	-
BC46	c[(bA)(bA)RKD]	Amide cyclic: 1-5	2.25	0.93
BC48	c[(bA)GRKD]	Amide cyclic: 1-5	1.89	1.01
BC49	c[(bA)(4aba)RKD]	Amide cyclic: 1-5	2.08	0.92
BC50	c[(4aba)(bA)RKD]	Amide cyclic: 1-5	2.93	0.89
BC51	c[(4aba)(4aba)RKD]	Amide cyclic: 1-5	2.62	0.75*
BC66	c[(bA)(k)RKD(f)]	Amide cyclic: 1-5	3.56	0.87
BC70	c[(bA)(k)RKD(1-D-Nal)]	Amide cyclic: 1-5	2.07	0.79
BC71	c[(bA)(k)RKD(2-D-Nal)]	Amide cyclic: 1-5	3.48	0.79*
BC72	c[(bA)(o)RKD(f)]	Amide cyclic: 1-5	1.81	0.96
BC74	c[(bA)(k)(Fguan)KD(f)]	Amide cyclic: 1-5	2.48	1.02
BC75	c[(bA)(k)RKD(D-Bip)]	Amide cyclic: 1-5	1.90	1.03
BC81	c[(2233tmpa) (k)RKD(2-D-Nal)]	Amide cyclic: 1-5	2.59	0.82
BC83	c[(bA) (k)RKD (D-2Anth)]	Amide cyclic: 1-5	2.15	0.85
BC84	c[(bA)(k)RKD(w)]	Amide cyclic: 1-5	2.65	0.79*

For clarity of presentation, data were normalized with that of non-treated (VEGF only) cells Data are expressed as mean ± standard error of the mean. * $p < 0.05$ indicates a significant decrease of cell viability by ISM-derived peptide analogues.

3.4. BC71 Binds to GRP78

Using SPR, we show that BC71 binds GRP78 with a higher affinity (K_d of 211 μM) in our experimental condition than a Kringle 5 peptide, a previously reported ligand for cell-surface GRP78 (k5-1, K_d of 8.6 mM) (Fig. 4a) [6].

To map the binding sites of BC71 on GRP78, we used recombinant $GRP78_{26–410}$ containing the active N-terminal ATPase domain and performed amide hydrogen-deuterium exchange mass spectrometry (HDXMS) [10]. The interactions of the product nucleotide ADP with GRP78 ATPase domain were first mapped by HDXMS. A difference plot of ADP-bound GRP78 and ligand-free GRP78 showed decreased deuterium exchange in the pink region (known ADP binding sites from the crystal structure of ADP-$GRP78_{26–410}$) and the blue region (not identified in previous crystal structure of ADP-$GRP78_{26–410}$) (Fig. 4b). Hence, this region (243–266) likely represents allosteric conformational changes upon ADP binding. Binding of BC71 alone interestingly showed global increases in deuterium exchange across GRP78 (Fig. 4c), indicated by positive magnitude differences in the difference plot for BC71-bound GRP78 relative to GRP78 alone. The difference plot of ADP-BC71-bound GRP78 vs. ADP-bound GRP78 (Fig. 4d) highlights the effects of BC71 addition to ADP-bound GRP78. One region, i.e. peptide spanning residues 244–257 (highlighted in orange), displayed time-dependent decreases in deuterium exchange upon BC71 addition. This indicated that BC71 was binding to the ADP-bound GRP78 at this site, slowing deuterium exchange in this region (represented as orange spheres in Fig. 4h). Since region 244–257 is not involved in ADP binding (based on crystal structure of ADP-$GRP78_{26–410;}$ PDB ID: 3IUC), therefore BC71 binding site doesn't overlap with ADP binding site in GRP78.

ADP is the product of ATP hydrolysis performed by GRP78 ATPase, and we next set out to test the effects of substrate ATP on BC71 binding to $GRP78_{26–410}$. We thus examined BC71-GRP78 interactions in the presence of the non-hydrolysable ATP analog AMPPNP. In the difference plot of AMPPNP-BC71-bound GRP78 versus AMPPNP-bound GRP78 (Fig. 4e), the magnitude of both positive and negative differences in exchange was enhanced in comparison with ADP-bound GRP78 (Fig. 4d). A greater protection from deuterium exchange at the 244–257 locus is observed (represented as orange spheres in Fig. 4h), suggesting a stronger binding interaction of BC71 with GRP78 in the presence of AMPPNP. Enhanced conformational dynamics mediated upon BC71 binding was also inferred from the larger magnitude of differences in exchange across the N-terminal region of GRP78 (Fig. 4e), indicating AMPPNP interactions with GRP78 may facilitate a relatively greater stability of BC71 binding pocket, while enhancing conformational dynamics in other parts of the protein. Thus, BC71 binds to both ADP-bound and ATP-bound GRP78 at 244–257 region. However, it preferentially interacts with ATP-bound GRP78 over the ADP-bound state, and this may be linked to the disruption of GRP78 function by BC71 in the presence of cellular ATP.

3.5. BC71 Targets and Suppresses 4 T1 Breast Cancer Growth in Mice

To investigate if BC71 can selectively target cell-surface GRP78 in tumor cells and tumor vessel endothelial cells, we conducted mouse imaging experiment using near-infrared fluorescent dye cyanine 7 labeled BC71 (Cy7-BC71) or mutated control peptide GR35 (Cy7-GR35). Mice bearing subcutaneous 4 T1 tumor were intravenously injected with Cy7-BC71 or Cy7-GR35 at a dose of 1 nmol/mouse and imaged at various time points post injection (p.i., 0 h, 2 h, 12 h, 24 h, 48 h and 72 h). Cy7-BC71 showed prominent accumulation in tumor from 2 h p.i., and a large amount of the peptide still remained in the tumor at 72 h p.i. when the experiment was terminated (Fig. 5, a & b). In comparison, Cy7-GR35 showed very low level of fluorescent signal in tumor from 24 h onwards (Fig. 5, a & b). Similarly, Cy7 dye alone showed minimum fluorescent signal in tumor at 48 h and 72 h p.i. Whole mouse imaging plus ex vivo evaluation of the dissected organs and tumors at 72 h p.i. revealed that the clearance of the peptide is mainly through kidneys, bladder and liver (Fig. 5c and data not shown).

BC71 also triggers apoptosis in 4 T1 breast cancer cells in a caspase-8 dependent manner (Fig. 6a). However, BC71 does not induce 4 T1 cell necrosis (Fig. S3). Culturing 4 T1 cells under low glucose condition to induce cell stress also did not lead to BC71 triggering a higher level of apoptosis or necrosis, despite a significantly higher necrosis observed under this low glucose condition (Fig. S3). Intravenous administration of BC71 inhibited 4 T1 breast carcinoma growth in mice as a single agent at a dose of 250 μg/mouse (Fig. 6, b & c). A marked decrease in blood vessels nourishing the tumor was observed under BC71 treatment (Figs. 6 d and S4). Double staining of apoptotic cells (TUNEL) and ECs (endomucin) indicated that systemic BC71 treatment induced massive apoptosis in tumor tissue and significantly reduced tumor angiogenesis (Fig. 6 e). Meanwhile, we did not observe any body weight loss or dysfunction of liver and kidney (Fig. S5). Similarly, intravenous administration of peptide BC51 at the same dose also suppressed 4 T1 tumor growth in mice, with obviously reduced blood vessels nourishing the tumor (Fig. S6).

4. Discussions

In this work, we report a series of proapoptotic cyclic peptides targeting cell-surface GRP78. The core functioning motif of these ISM-

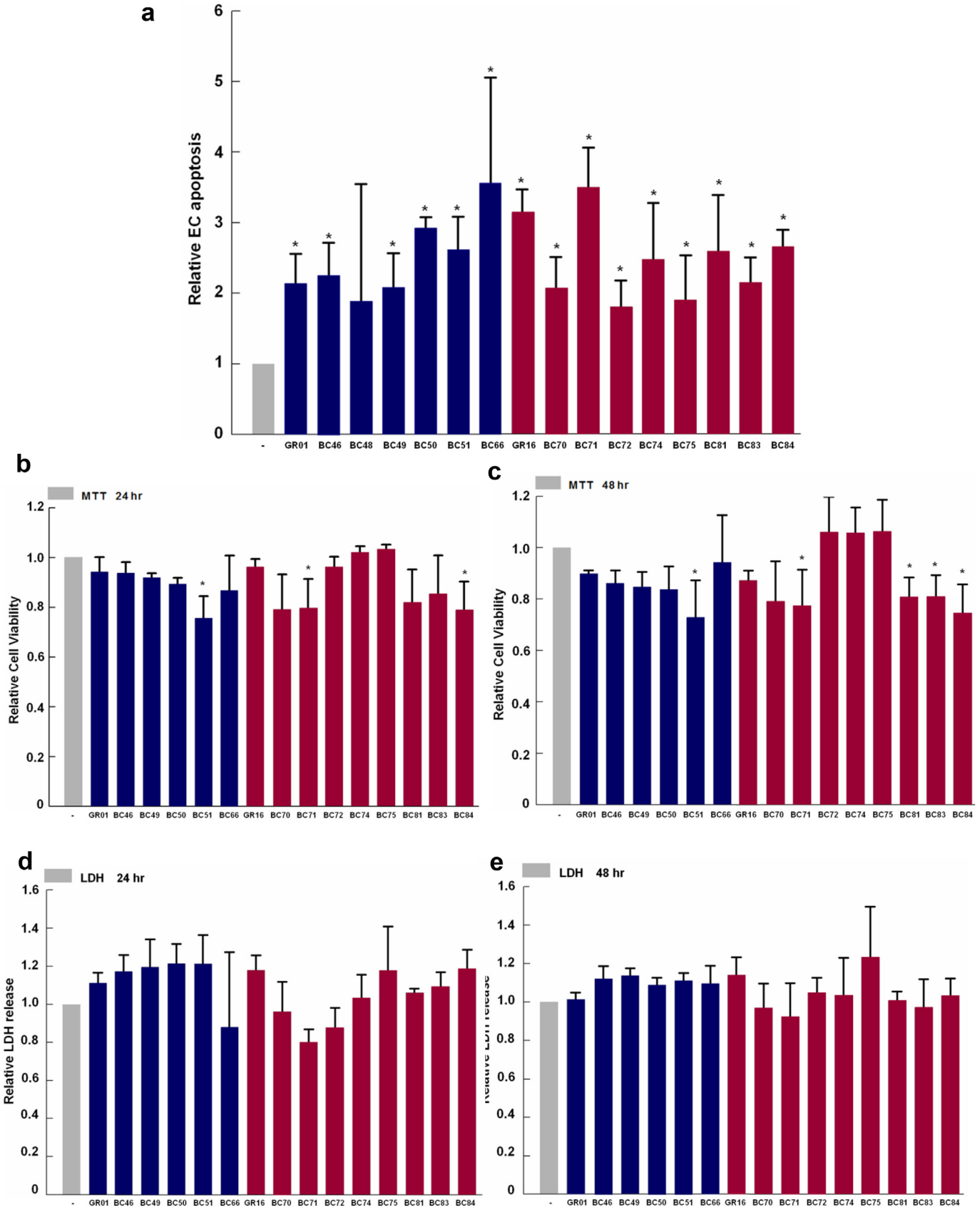

derived peptides is RKD. BC71, the most potent peptide analogue, suppressed 4 T1 breast cancer xenograft in mice as a single agent when administered intravenously.

We show that BC71 induces HUVEC apoptosis by interacting with cell-surface GRP78 but not αvβ5 integin (Fig. 2). Similar to ISM, BC71 targets the N-terminal region of GRP78 to induce apoptosis [4]. BC71

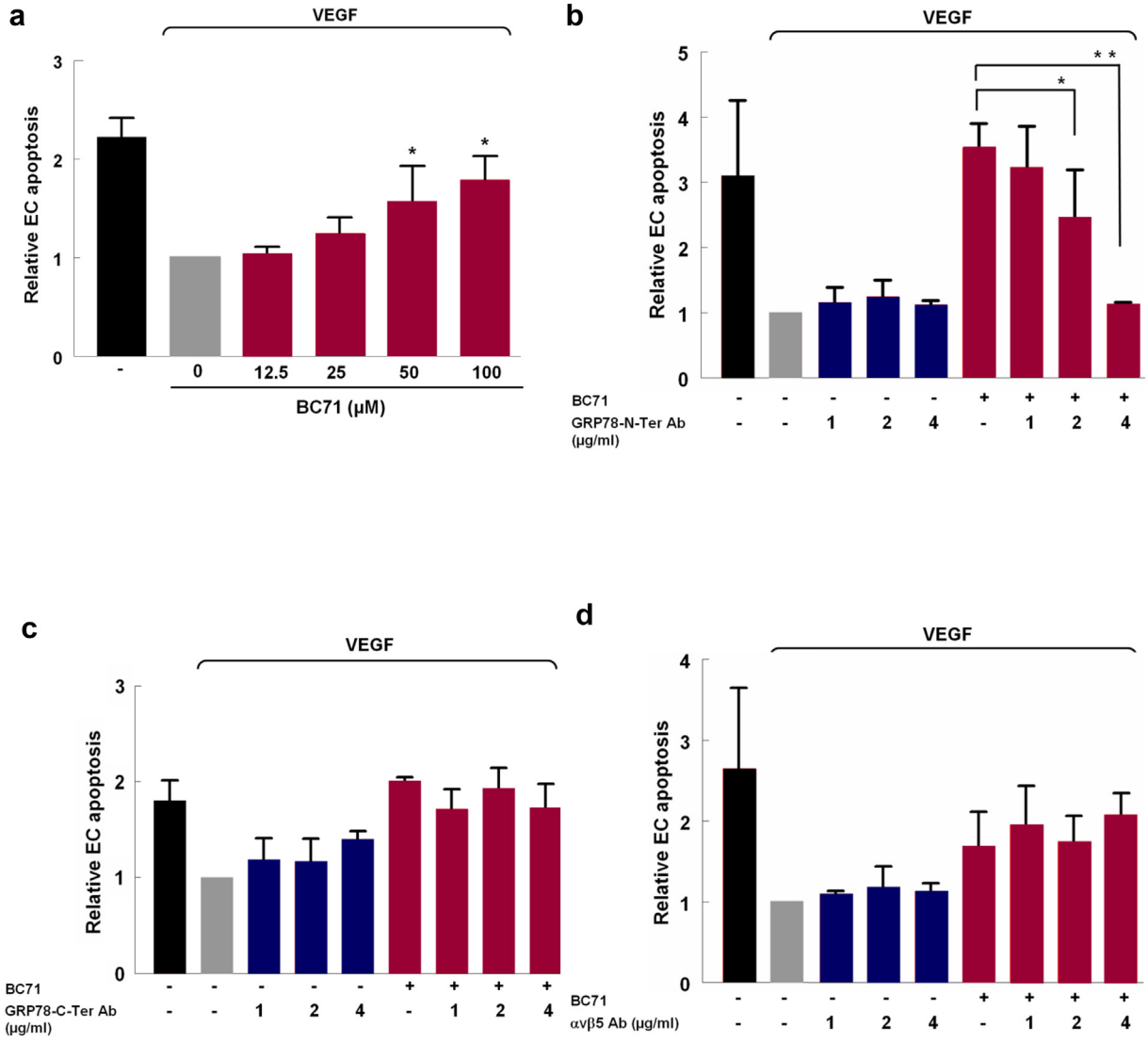

Fig. 2. BC71 targets cell-surface GRP78 but not αvβ5 integrin to induce apoptosis. (a) BC71 induces HUVECs apoptosis in a dose-dependent manner. HUVECs were treated with BC71 (concentration range: 12.5, 25, 50, 100 μM) for 24 h and apoptosis was determined using the cell death ELISA kit (Roche). (b) Anti-GRP78 N-terminal domain antibody blocked the apoptosis function of BC71 in a dose-dependent manner. The apoptosis of the combined treatment with increasing amount of anti-GRP78 N-terminal domain antibody and 100 μM BC71 for 24 h was measured using the Cell Death Detection ELISA. (c) Anti-GRP78 C-terminal domain antibody and (d) anti-αvβ5 antibody did not block BC71 induced apoptosis. For clarity of presentation, data were normalized with that of non-treated (VEGF only) cells, which was set as 1. Data are expressed as mean ± standard error of the mean. The results are representative of at least three independent experiments. Statistical significance was determined using ANOVA. *P < 0.05; **P < 0.01, n ≥ 3.

is modified from peptide GR16, a head-to-tail cyclic pentapeptide harboring the native sequence of KRKDF in the AMOP domain of ISM. Modification of two terminal amino acids to D-lysine and 2-naphthyl-D-alanine followed by head-to-tail cyclization via β-alanine lead to BC71 which presented enhanced binding to GRP78 (K_d of 211 μM) and more potent proapoptotic activity. Notably, under the same SPR assay condition, k5-1 (PRKLYDY), a previously reported GRP78 peptide ligand derived from kringle 5 (k5) of human plasminogen, only presented a K_d of 8.6 mM [6]. k5-1 has been shown to be equally effective comparing to k5 in inhibiting VEGF-stimulated migration of human microvascular endothelial cells (HMVEC) [6].

GRP78 is an ATPase and its ATPase domain binds with high affinity to both ATP and ADP (Kd in nM) [10]. HDXMS studies revealed that BC71 binds to both ADP-bound and AMPPNP-bound (ATP-bound) GRP78 via the same region of residues 244–257 (Fig. 4). Notably, BC71 binds much stronger to AMPPNP-bound GRP78, hence potentially disrupt ATP-bound GRP78 function in cells.

Our results indicate that BC71 induces HUVECs and 4 T1 breast cancer cells apoptosis via activation of caspase-8 and induction of p53 protein in treated cells (Fig. 3). Interestingly, inhibiting NF-κB signaling also potently quenched BC71 induced apoptosis (Fig. S7). How NF-κB signaling is linked to caspase-8 and p53 pathways

Fig. 1. RKD containing cyclic peptides derived from the AMOP domain of ISM trigger apoptosis but not necrosis of HUVECs in culture. (a) GR01 and GR16 and peptide analogues derived from them induce apoptosis in HUVECS. Cells were treated with 100 μM of GR01, GR16 and analogues for 24 h and apoptosis were determined with Cell Death Detection ELISA (Roche). GR16, BC66, BC70, BC71, BC72, BC74, BC75, BC81, BC83 and BC84 induced apoptosis with relative fold change over 1.4. (b, c) BC51, BC71 and BC84 reduced HUVEC viability at 24 h post-treatment. HUVECs were treated with 100 μM of for 24 h and 48 h treatment. MTT assay was used to determine the cell viability. Significant viability reduction is indicated by *. (d, e) No necrosis was induced by any peptide analogue. The necrotic effects of peptide analogues at 100 μM were determined at 24 h and 48 h post-treatment using the LDH secretion assay in HUVECs. For clarity of presentation, data were normalized with that of non-treated (VEGF only) cells, which was set as 1. Data are expressed as mean ± standard error of the mean. The results are representative of at least three independent experiments. Statistical significance was determined using ANOVA. *P < 0.05; **P < 0.01, n ≥ 3.

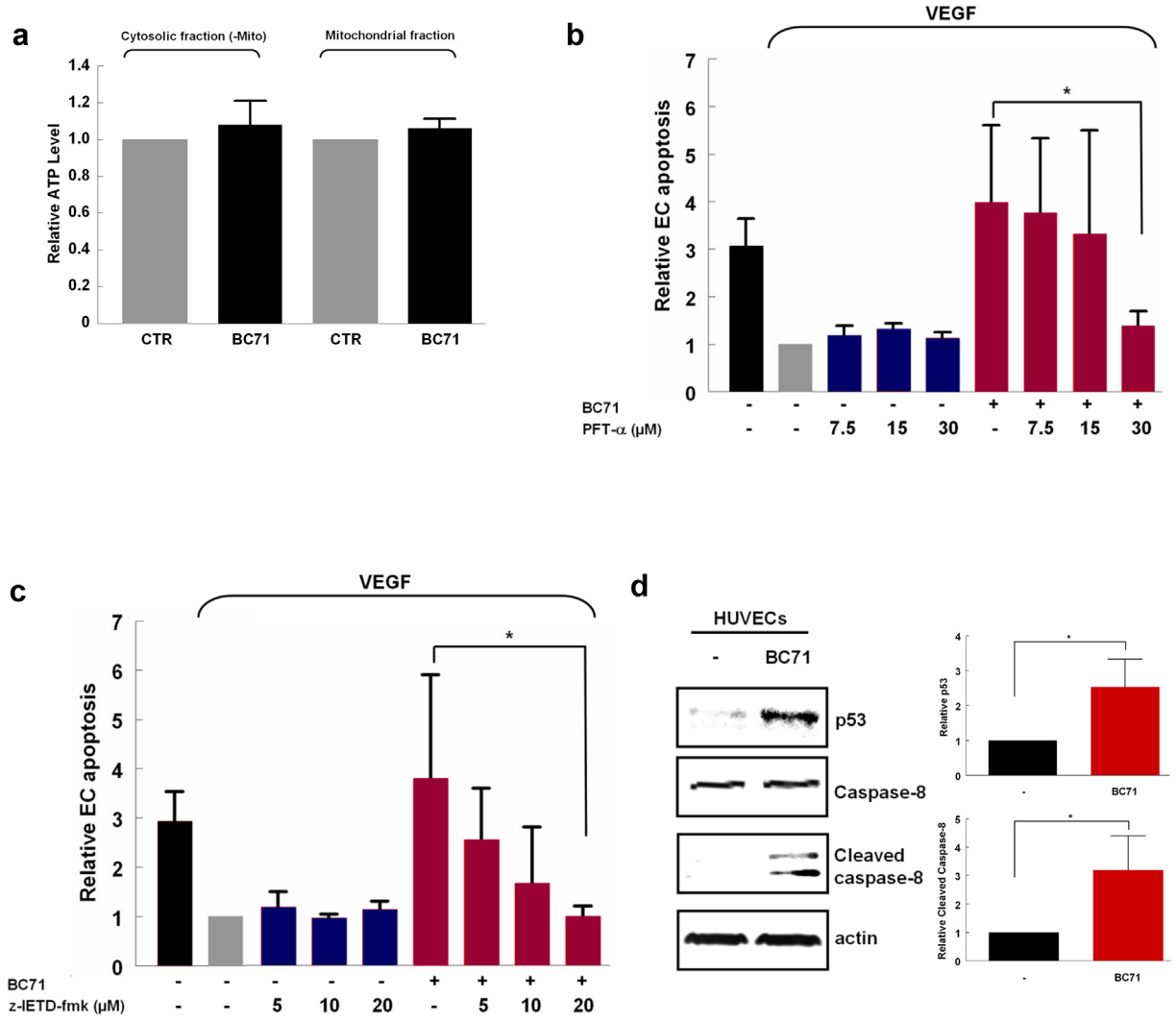

Fig. 3. BC71 induced caspase-8 and p53-mediated apoptosis signaling pathways. (a) BC71 does not influence ATP level in cytosol and mitochondria of HUVECs. HUVECs were treated with 100 μM BC71 for 24 h, mitochondrial and cytosolic (without mitochondria) fractions were being collected and were measured by ATP colorimetric assay. (b) Caspase-8 inhibitor dose-dependently suppressed BC71-induced apoptosis. HUVECs were treated with 5, 10, or 20 μM of z-IETD-fmk together with 100 μM BC71 for 24 h and apoptosis determined as described above. (c) p53 inhibitor dose-dependently suppressed BC71-induced apoptosis. HUVECs were co-treated with 7.5, 15, or 30 μM of PFT-α together with 100 μM BC71 for 24 h and apoptosis wrere then determined. For clarity of presentation, data were normalized with that of non-treated (VEGF only) cells, which was set as 1. (d) HUVECs were treated with 100 μM BC71 for 24 h, and the changes in p53 and cleaved-caspase 8 levels were analyzed with western blots. The quantitative data obtained for these proteins are presented. Data are expressed as mean ± standard error of the mean. Statistical significance was determined using ANOVA. *P < 0.05; **P < 0.01, n = 3.

under BC71 treatment will need to be further investigated in future.

More and more peptide drugs have been approved by the FDA [15]. Compared with recombinant proteins and antibodies, peptide drugs present low immunogenicity, can be chemically synthesized in large-scale and have better shelf lives. Compared to small molecules, peptides are metabolized to harmless amino acids and do not accumulate in tissues and organs, thus significantly reducing potential side effects and long-term toxicity [8]. The limitations of peptide drugs are their low metabolic stability and high cost of large scale synthesis. However, in recent years, technologies to enhance the stability of peptides and scaling up of peptide synthesis have improved [8, 32]. Tumor-targeting peptides have also been explored as delivery vehicles to deliver anticancer drugs to specific tumors ([14]; [20]). Since BC71 possess the ability to target tumor in mice via cell-surface GRP78 (Fig. 5), this peptide also has the potential to be conjugated to chemotherapy drugs to enhance drug delivery to tumors and anticancer efficacy.

Previously, a peptidomimetic proapoptotic ligand of GRP78, BMTP-78, composed by a GRP78-binding peptide fused to a proapoptotic enantiomer, suppressed tumor growth and prolongs animal survival in several preclinical tumor models [1, 22]. However, BMTP-78 caused unexpected toxicity in nonhuman primates and cannot be pursued further

Fig. 4. Binding and interactions of BC71 with GRP78 determined by SPR and HDXMS. (a) SPR sensograms showing the binding of peptides BC71 at different concentrations to GRP78 protein immobilized on NTA chip. Left panel: k5-1 peptide; right panel: BC71 peptide. The K_d values were globally fitted with Rmax = 13.3 (2) using Scrubber 2.0 software. The response was normalized for the molecular weight of each peptide and for the immobilization level achieved by GRP78 protein. (b–e) HDXMS analyses of BC71 interaction with $GRP78_{26–410}$. Difference plots of HDXMS data for the protein in (b) ADP-bound and Apo state, (c) BC71-bound and Apo state, (d) ADP-BC71-bound and ADP-bound state, (e) AMPPNP-BC71-bound state and AMPPNP-bound state. Peptides spanning the known ADP-interacting residues are highlighted in pink and additional regions showing reduced deuterium exchange upon ADP-binding are highlighted in blue. The peptide showing reduced deuterium exchange upon BC71 binding in both ADP-BC71-bound state and AMPPNP-BC71-bound state is highlighted in orange. (f, g, h) BC71-GRP78 interacting region identified by HDXMS presented in crystal structure of $GRP78_{26–410}$. ADP is shown as green spheres. Residues in pink spheres represent the increased deuterium exchange region in the presence of BC71. Residues in orange (244–257) shows reduced deuterium uptake when BC71 is bound with GRP78-ADP or GRP78-AMPPMP.

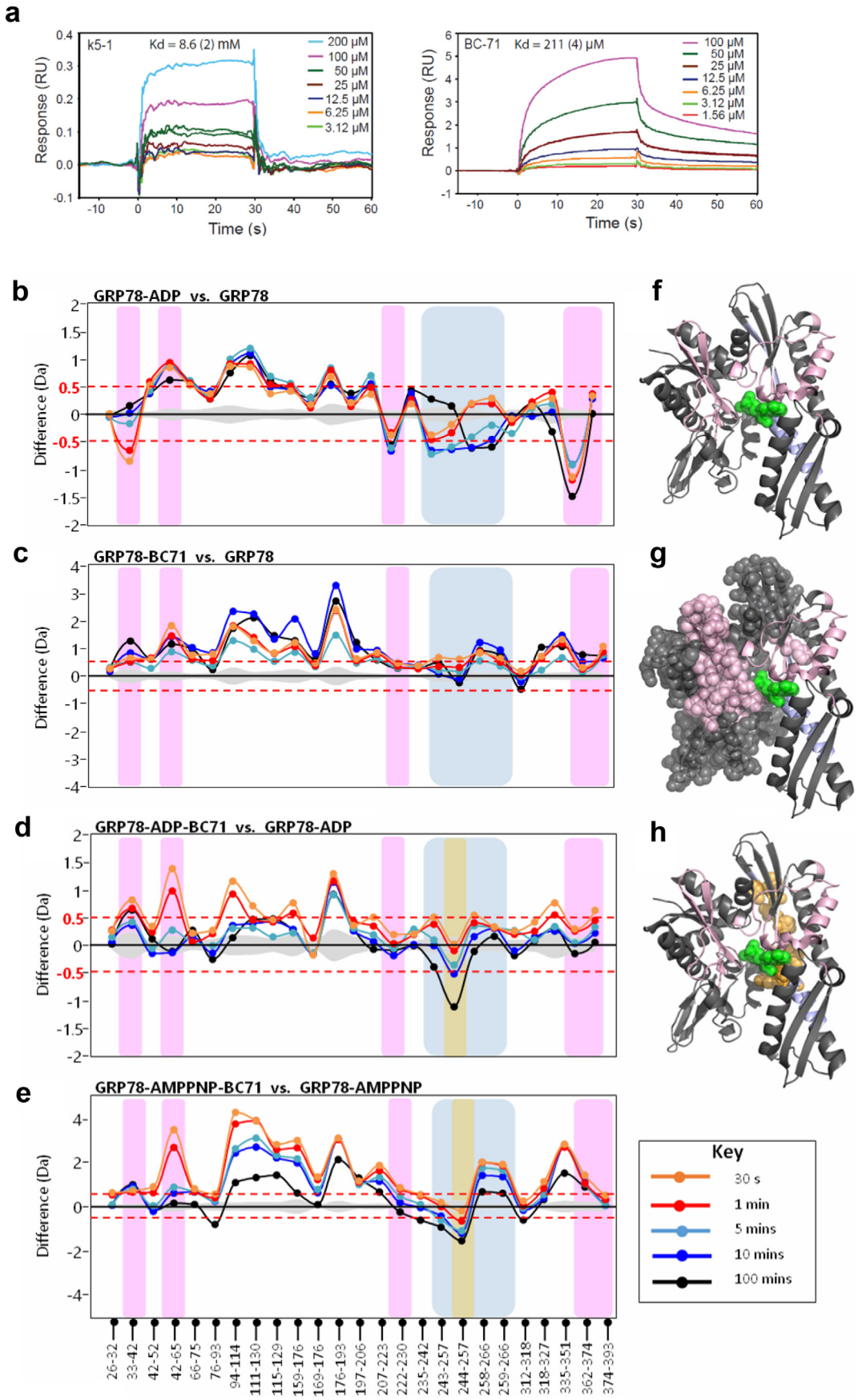
a
k5-1
Kd = 8.6 (2) mM
200 μM
100 μM
50 μM
25 μM
12.5 μM
6.25 μM
3.12 μM
Response (RU)
Time (s)
BC-71
Kd = 211 (4) μM
100 μM
50 μM
25 μM
12.5 μM
6.25 μM
3.12 μM
1.56 μM
Response (RU)
Time (s)
b
GRP78-ADP vs. GRP78
Difference (Da)
c
GRP78-BC71 vs. GRP78
Difference (Da)
d
GRP78-ADP-BC71 vs. GRP78-ADP
Difference (Da)
e
GRP78-AMPPNP-BC71 vs. GRP78-AMPPNP
Difference (Da)
26-32
33-42
42-52
42-65
66-75
76-93
94-114
111-130
115-129
159-176
169-176
176-193
197-206
207-223
222-230
235-242
243-257
244-257
258-266
259-266
312-318
318-327
335-351
362-374
374-393
f
g
h
Key
30 s
1 min
5 mins
10 mins
100 mins

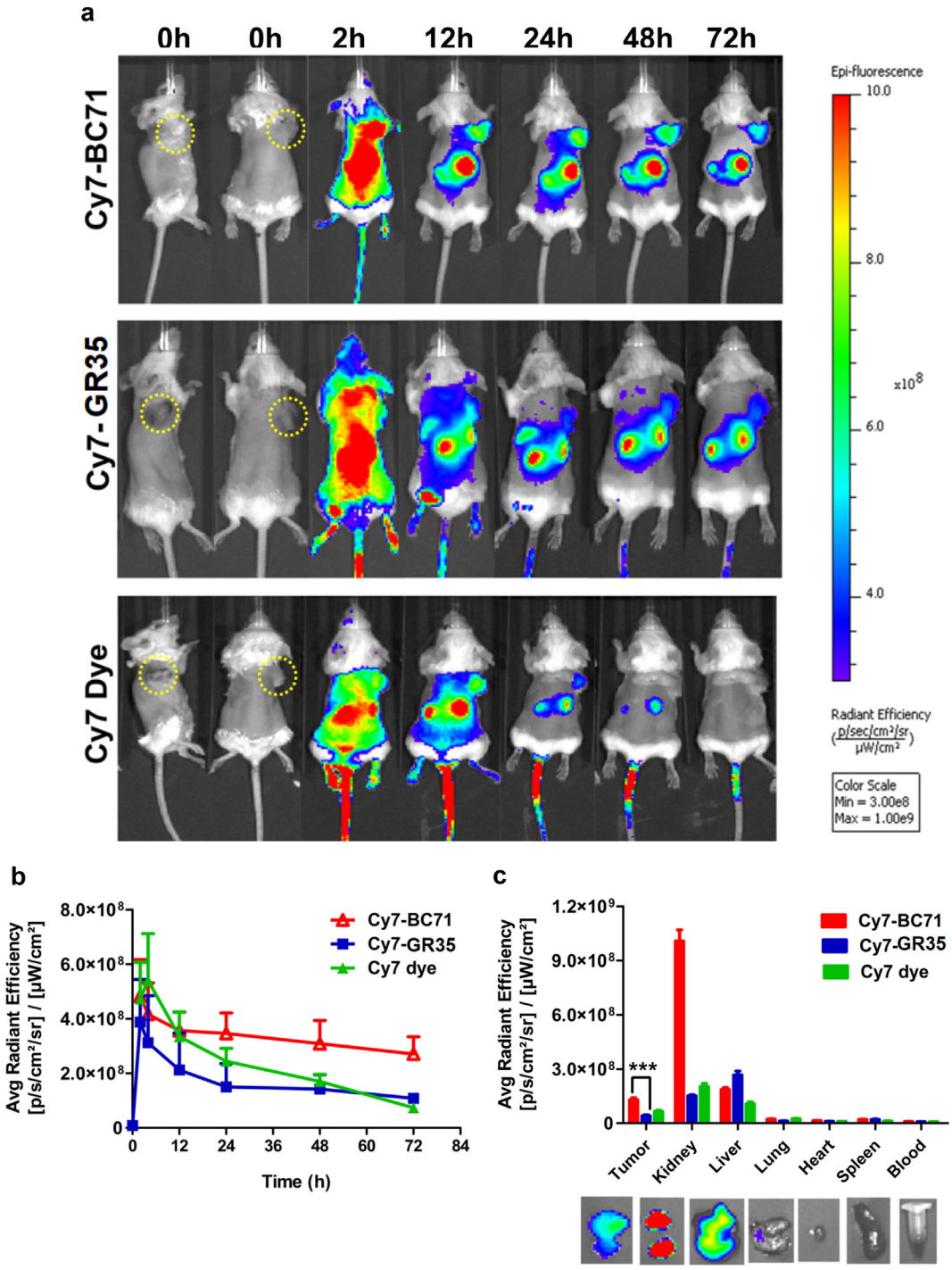

Fig. 5. Cy7-BC71 home to 4 T1 breast tumor in subcutaneous xenograft mouse tumor model. (a) Comparison of whole-body near-infrared fluorescence of subcutaneous 4 T1 tumor bearing mice injected with 1 nmol of Cy7-BC71, Cy7-GR35 or Cy7 dye alone at 2 h, 12 h, 24 h, 48 h, 72 h p.i. The position of tumor is indicated with white arrows and all images are normalized to the same scale. (b) Quantification of fluorescence intensity of the tumor as a function of time after the injection of the Cy7-BC71, Cy7-GR35 or Cy7 dye **(c)** Ex-vivo fluorescence intensity of various organs at 72 h p.i. The data is represented as Mean ± S.D. (n = 5 for each group), **p = 0.0073.

as drugs [29]. Compared to BMTP-78, BC71 is a much smaller cyclic peptide with a single motif mediating both GRP78 binding and proapoptotic activity. BC71 is also less potent in inducing apoptosis of cultured HUVECs (data not shown), features that may potentially be more advantageous for it to function as an imaging agent or drug carrier for cancer therapy in vivo.

Small cyclic peptides, such as the integrin targeting RGD peptide cilengitide, has previously reached phase II clinical trials for the treatment of glioblastoma [19, 27]. A radiolabeled RGD peptide has also been used for PET imaging of αvβ3 integrin as an indicator for effectiveness of anti-angiogenesis therapy [3]. As a single agent at 250 μg/mouse, cilengitide was reported to be ineffective in suppressing human HBT 3477 breast cancer in nude mice. However, it enhanced the efficacy of radioimmunotherapy in a combination therapy study [2]. In comparison, BC71 at the same dose (250 μg/mouse) effectively inhibited 4 T1 breast cancer growth in syngeneic mice as a single agent (Fig. 6).

In summary, we report here a series of novel cyclic peptides that target cell-surface GRP78. The most potent peptide, BC71, suppressed

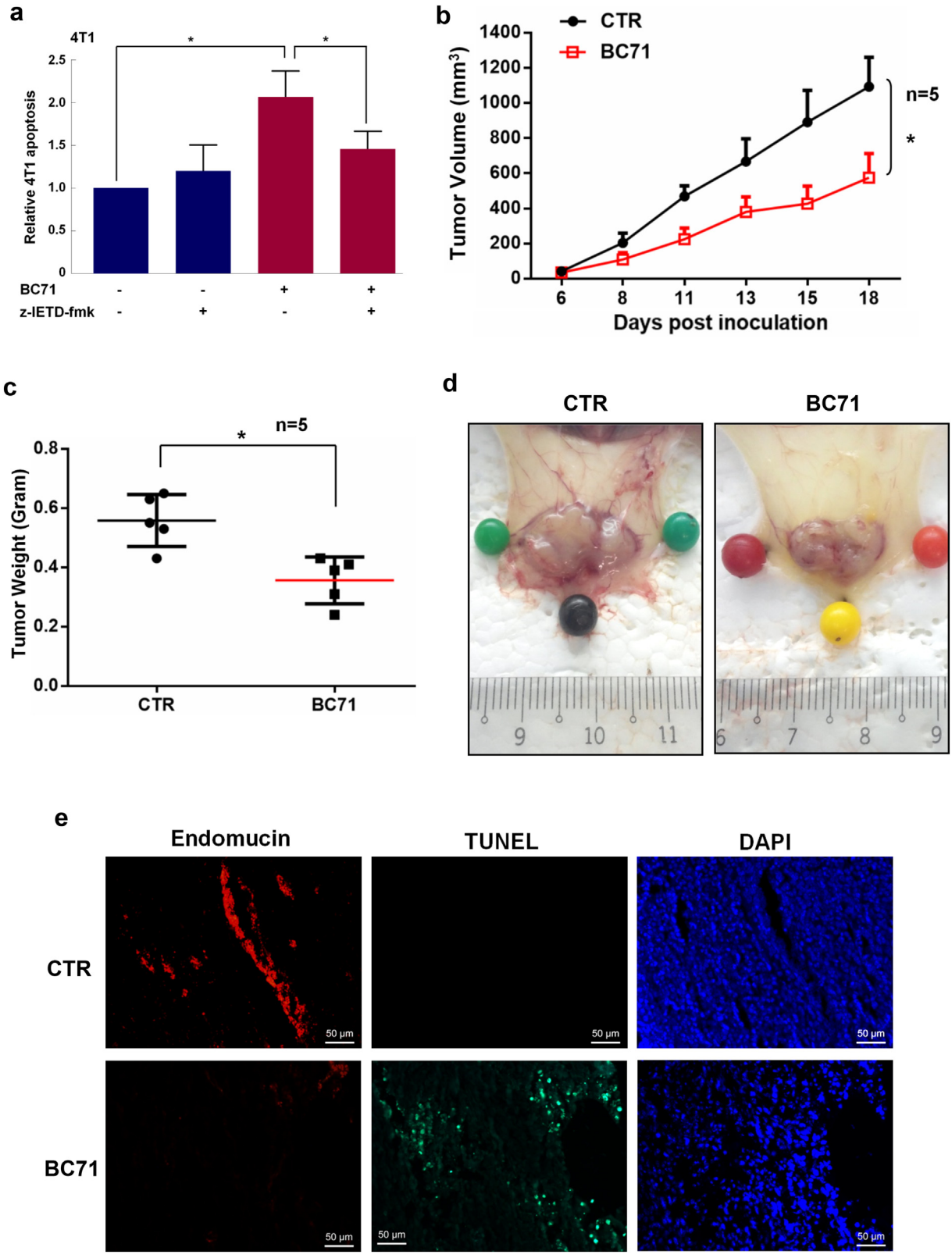

Fig. 6. Systemically delivered BC71 suppressed 4 T1 breast cancer growth in mice. (a) 4 T1 cells were co-treated with 40 μM of z-IETD-fmk together with 100 μM BC71 for 24 h and apoptosis were then determined. For clarity of presentation, data were normalized with that of vehicle control cells, which was set as 1. (b–d) BC71 inhibits 4 T1 breast carcinoma growth in mice when delivered intravenously. Tumor weight is at the end of the experiment (day 18). Groups consisted of control mice receiving PBS (non-treatment) or treatment of 250 μg/mouse BC71 through tail vein injection every other day from day 0 (date of inoculation) to 18. n = 5. (e) Representative immunofluorescence staining for endomucin (red, endothelial cells) and TUNEL (green, apoptotic cells) in tumor sections. Cell nuclei were counterstained with DAPI. Scale bars represent 50 μm.

tumor growth in mice and targeted tumor via GRP78 when administered intravenously. We believe BC71 can serve as a valuable prototype molecule for further development into GRP78 targeted peptidomimetic anticancer therapeutics. Radiolabeled BC71 can also be used in PET imaging to determine cell-surface GRP78 levels for cancer prognosis. Nevertheless, as BC71 binds to GRP78 at micromolar affinity, higher affinity derivatives of BC71 may need to be developed to serve as effective PET imaging probe for clinical applications.

Funding Sources

This work is funded by grants awarded to Ruowen Ge from the Singapore National Medical Research Council (NMRC/CBRG/0062/2014) and Ministry of Education (R-154-000-640-112).

Conflict of Interest

The authors declare no conflict of interest.

Author Contributions

Ruowen Ge conceived and directed this research; Chieh Kao and Mo Chen carried out cell culture based biological studies and mouse tumorigenesis studies; Ritu Chandna performed the Cy7-BC71 tumor targeting study in mice and generated recombinant GRP78 protein; Abhijeet Ghode and Ganesh S. Anand carried out HDXMS investigations; Charlotte Dsouza, Minjun Wang and Zhonglian Cao carried out SPR experiments; Andreas Larsson and Siau Hoi Lim provided technical support for SPR study; Yizhun Zhu contributed material for this project; Chieh Kao, Ritu Chandna, Abhijeet Ghode, Ganesh S. Anand, Charlotte Dsouza and Ruowen Ge wrote the manuscript.

Research in Context

Cell-surface GRP78 is preferentially overexpressed in aggressive, metastatic and chemoresistant cancers. It is a recently emerged target for anticancer therapy and an indicator for cancer prognosis. We developed cyclic RKD peptide analogues that specifically targets cell-surface GRP78 and trigger apoptosis. One such peptide BC71 home to tumor and suppressed tumor growth in mice as a single agent via inhibiting tumor angiogenesis and triggering intra-tumor apoptosis. BC71 is thus a valuable prototype molecule that has the potential to be further developed into anticancer therapeutic.

Acknowledgments

We would like to thank Brian Chia of the Experimental Therapeutics Centre, Agency for Science, Technology and Research (A*STAR) for help in designing the peptides and provide comments for the manuscript.

Appendix A. Supplementary Data

Supplementary data to this article can be found online at https://doi.org/10.1016/j.ebiom.2018.06.004.

References

[1] Arap MA, Lahdenranta J, Mintz PJ, Hajitou A, Sarkis AS, Arap W, et al. Cell surface expression of the stress response chaperone GRP78 enables tumor targeting by circulating ligands. Cancer Cell 2004;6:275–84.
[2] Burke PA, Denardo SJ, Miers LA, Lamborn KR, Matzku S, Denardo GL. Cilengitide targeting of alpha(v)beta(3) integrin receptor synergizes with radioimmunotherapy to increase efficacy and apoptosis in breast cancer xenografts. Cancer Res 2002;62:4263–72.
[3] Chen H, Niu G, Wu H, Chen X. Clinical application of radiolabeled RGD peptides for PET imaging of integrin alphavbeta3. Theranostics 2016;6:78–92.
[4] Chen M, Zhang Y, Yu VC, Chong YS, Yoshioka T, Ge R. Isthmin targets cell-surface GRP78 and triggers apoptosis via induction of mitochondrial dysfunction. Cell Death Differ 2014;21:797–810.
[5] Croce CM, Reed JC. Finally, an apoptosis-targeting therapeutic for Cancer. Cancer Res 2016;76:5914–20.
[6] Davidson DJ, Haskell C, Majest S, Kherzai A, Egan DA, Walter KA, et al. Kringle 5 of human plasminogen induces apoptosis of endothelial and tumor cells through surface-expressed glucose-regulated protein 78. Cancer Res 2005;65:4663–72.
[7] Fesik SW. Promoting apoptosis as a strategy for cancer drug discovery. Nat Rev Cancer 2005;5:876–85.
[8] Fosgerau K, Hoffmann T. Peptide therapeutics: current status and future directions. Drug Discov Today 2015;20:122–8.
[9] Hanahan D, Weinberg RA. Hallmarks of cancer: the next generation. Cell 2011;144:646–74.
[10] Hughes SJ, Antoshchenko T, Chen Y, Lu H, Pizarro JC, Park HW. Probing the ATP site of GRP78 with nucleotide triphosphate analogs. PLoS One 2016;11:e0154862.
[11] Khan KH, Blanco-Codesido M, Molife LR. Cancer therapeutics: targeting the apoptotic pathway. Crit Rev Oncol Hematol 2014;90:200–19.
[12] Kim Y, Lillo AM, Steiniger SC, Liu Y, Ballatore C, Anichini A, et al. Targeting heat shock proteins on cancer cells: selection, characterization, and cell-penetrating properties of a peptidic GRP78 ligand. Biochemistry 2006;45:9434–44.
[13] Kumar S, Sharghi-Namini S, Rao N, Ge R. ADAMTS5 functions as an anti-angiogenic and anti-tumorigenic protein independent of its proteoglycanase activity. Am J Pathol 2012;181:1056–68.
[14] Laakkonen P, Vuorinen K. Homing peptides as targeted delivery vehicles. Integr Biol (Camb) 2010;2:326–37.
[15] Lau JL, Dunn MK. Therapeutic peptides: historical perspectives, current development trends, and future directions. Bioorg Med Chem 2018;26(10):2700–7 (published online in 2017).
[16] Lee AS. Glucose-regulated proteins in cancer: molecular mechanisms and therapeutic potential. Nat Rev Cancer 2014;14:263–76.
[17] Li J, Lee AS. Stress induction of GRP78/BiP and its role in cancer. Curr Mol Med 2006;6:45–54.
[18] Liu R, Li X, Gao W, Zhou Y, Wey S, Mitra SK, et al. Monoclonal antibody against cell surface GRP78 as a novel agent in suppressing PI3K/AKT signaling, tumor growth, and metastasis. Clin Cancer Res 2013;19:6802–11.
[19] Manegold C, Vansteenkiste J, Cardenal F, Schuette W, Woll PJ, Ulsperger E, et al. Randomized phase II study of three doses of the integrin inhibitor cilengitide versus docetaxel as second-line treatment for patients with advanced non-small-cell lung cancer. Invest New Drugs 2013;31:175–82.
[20] Maurizio Roveri MB, Lerouxa Jean-Christophe, Luciani Paola. Peptides for tumor specific drug targeting: state of the art and beyond. J Mater Chem B 2017;5:4348–64.
[21] Mcfarland BC, Stewart Jr J, Hamza A, Nordal R, Davidson DJ, Henkin J, et al. Plasminogen kringle 5 induces apoptosis of brain microvessel endothelial cells: sensitization by radiation and requirement for GRP78 and LRP1. Cancer Res 2009;69:5537–45.
[22] Miao YR, Eckhardt BL, Cao Y, Pasqualini R, Argani P, Arap W, et al. Inhibition of established micrometastases by targeted drug delivery via cell surface-associated GRP78. Clin Cancer Res 2013;19:2107–16.
[23] Rasche L, Duell J, Morgner C, Chatterjee M, Hensel F, Rosenwald A, et al. The natural human IgM antibody PAT-SM6 induces apoptosis in primary human multiple myeloma cells by targeting heat shock protein GRP78. PLoS One 2013;8:e63414.
[24] Rasche L, Menoret E, Dubljevic V, Menu E, Vanderkerken K, Lapa C, et al. A GRP78-directed monoclonal antibody recaptures response in refractory multiple myeloma with extramedullary involvement. Clin Cancer Res 2016;22:4341–9.
[25] Roller C, Maddalo D. The molecular chaperone GRP78/BiP in the development of Chemoresistance: mechanism and possible treatment. Front Pharmacol 2013;4:10.
[26] Sato M, Yao VJ, Arap W, Pasqualini R. GRP78 signaling hub a receptor for targeted tumor therapy. Adv Genet 2010;69:97–114.
[27] Scaringi C, Minniti G, Caporello P, Enrici RM. Integrin inhibitor cilengitide for the treatment of glioblastoma: a brief overview of current clinical results. Anticancer Res 2012;32:4213–23.
[28] Shrestha-Bhattarai T, Rangnekar VM. Cancer-selective apoptotic effects of extracellular and intracellular Par-4. Oncogene 2010;29:3873–80.
[29] Staquicini DI, D'Angelo S, Ferrara F, Karjalainen K, Sharma G, Smith TL, et al. Therapeutic targeting of membrane-associated GRP78 in leukemia and lymphoma: preclinical efficacy in vitro and formal toxicity study of BMTP-78 in rodents and primates. Pharmacogenomics J 2018;18(3):436–43 (published online in 2017).
[30] Ulianich L, Insabato L. Endoplasmic reticulum stress in endometrial cancer. Front Med (Lausanne) 2014;1:55.
[31] Virrey JJ, Dong D, Stiles C, Patterson JB, Pen L, Ni M, et al. Stress chaperone GRP78/BiP confers chemoresistance to tumor-associated endothelial cells. Mol Cancer Res 2008;6:1268–75.
[32] Vlieghe P, Lisowski V, Martinez J, Khrestchatisky M. Synthetic therapeutic peptides: science and market. Drug Discov Today 2010;15:40–56.
[33] Wang SH, Lee AC, Chen IJ, Chang NC, Wu HC, Yu HM, et al. Structure-based optimization of GRP78-binding peptides that enhances efficacy in cancer imaging and therapy. Biomaterials 2016;94:31–44.
[34] Watson EC, Grant ZL, Coultas L. Endothelial cell apoptosis in angiogenesis and vessel regression. Cell Mol Life Sci 2017;74:4387–403.
[35] Wisniewska M, Karlberg T, Lehtio L, Johansson I, Kotenyova T, Moche M, et al. Crystal structures of the ATPase domains of four human Hsp70 isoforms: HSPA1L/Hsp70-hom, HSPA2/Hsp70-2, HSPA6/Hsp70B', and HSPA5/BiP/GRP78. PLoS One 2010;5:e8625.
[36] Xiang W, Ke Z, Zhang Y, Cheng GH, Irwan ID, Sulochana KN, et al. Isthmin is a novel secreted angiogenesis inhibitor that inhibits tumour growth in mice. J Cell Mol Med 2011;15:359–74.
[37] Zhang Y, Chen M, Venugopal S, Zhou Y, Xiang W, Li YH, et al. Isthmin exerts pro-survival and death-promoting effect on endothelial cells through alphavbeta5 integrin depending on its physical state. Cell Death Dis 2011;2:e153.